

Supporting Information for

Comparative Study of Magnetization Dynamics in Dinuclear Dysprosium Complexes Featuring Bridging Chloride or Trifluoromethanesulfonate Ligands

Corey P. Burns, Branford O. Wilkins, Courtney M. Dickie, Trevor P. Latendresse, Larry Vernier, Kuduva R. Vignesh, Nattamai S. Bhuvanesh, and Michael Nippe*

Department of Chemistry, Texas A&M University, 3255 TAMU, College Station, TX, 77843 (USA).

E-mail: nippe@chem.tamu.edu

Content

Experimental Details	S3-S6
Fig. S1 Packing diagram for 2 viewing along a-(left), b-(center), and c-axis (right).....	S7
Fig. S2 Plot of Magnetization vs. Field at 8-1.8 K for 1	S7
Fig. S3 Plot of Magnetization vs. H/T at 8-1.8 K for 1	S8
Fig. S4 Plot of Magnetization vs. Field at 8-1.8 K for 2	S8
Fig. S5 Plot of Magnetization vs. H/T at 8-1.8 K for 2	S9
Fig. S6 Plot of Magnetization vs. Field at 8-1.8 K for 3	S9
Fig. S7 Plot of Magnetization vs. H/T at 8-1.8 K for 3	S10
Fig. S8 Frequency dependence of the in-phase component (χ_M'') of the ac susceptibility of 1 under 0 Oe applied dc field in the temperature range 1.8 – 15 K.....	S10
Fig. S9 Frequency dependence of the in-phase component (χ_M') of the ac susceptibility of 2 under 0 Oe applied dc field in the temperature range 1.8 – 10 K.....	S11
Fig. S10 Frequency dependence of the out-of-phase component (χ_M'') of the ac susceptibility of 2 under 0 Oe applied dc field in the temperature range 1.8 – 10 K.....	S11
Fig. S11 Frequency dependence of the in-phase component (χ_M') of the ac susceptibility of 2 under 1000 Oe applied dc field in the temperature range 1.8 – 15 K.....	S12
Fig. S12 Frequency dependence of the out-of-phase component (χ_M'') of the ac susceptibility of 2 under 1000 Oe applied dc field in the temperature range 1.8 – 15 K.....	S12
Fig. S13 Frequency dependence of the in-phase component (χ_M') of the ac susceptibility of 3 under 0 Oe applied dc field in the temperature range 1.8 – 15 K.....	S13
Fig. S14 Cole-Cole plots under zero dc field for 1 . Solid lines are the best fits to the experimental data, obtained with the generalized Debye model.....	S13
Fig. S15 Cole-Cole plots under zero dc field for 3 . Solid lines are the best fits to the experimental data, obtained with the generalized Debye model.....	S14
Fig. S16 Frequency dependence of the in-phase component (χ_M') of the ac susceptibility of magnetically dilute 1 under 0 Oe applied dc field in the temperature range 2 – 14 K.....	S14
Fig. S17 Frequency dependence of the out-of-phase component (χ_M'') of the ac susceptibility of magnetically dilute 1 under 0 Oe applied dc field in the temperature range 2 – 14 K.....	S15
Fig. S18 Frequency dependence of the in-phase component (χ_M') of the ac susceptibility of magnetically dilute 3 under 0 Oe applied dc field in the temperature range 2.5 – 14 K.....	S15
Fig. S19 Frequency dependence of the out-of-phase component (χ_M'') of the ac susceptibility of magnetically dilute 3 under 0 Oe applied dc field in the temperature range 2.5 – 14 K.....	S16

Table S1. Crystallographic Data for 1 , 2 , and 3	S17
Table S2. Selected bond lengths and angles in molecular structures of 1 , 2 , and 3	S18
Table S3. Calculated g-tensor for Kramer's doublets of individual Dy sites in 1 , 2 , and 3	S19
Table S4. Lowest exchange doublets arising from magnetic coupling and the corresponding tunnel splitting and gz value of each doublet (g_x and $g_y = 0$) for complex 1 . Bold indicates doublet through which magnetic relaxation is expected to occur.	S20
Table S4. Lowest exchange doublets arising from magnetic coupling and the corresponding tunnel splitting and gz value of each doublet (g_x and $g_y = 0$) for complex 3 . Bold indicates doublet through which magnetic relaxation is expected to occur.....	S20
References	S21

Experimental Section

Materials and methods: Synthesis of 2,6-bis(methylenecyclopentadienyl)pyridine disodium salt, [(PyCp₂)Dy(μ-OTf)]₂ (**1**), [(PyCp₂)Dy(thf)(OTf)] (**2**), and [(PyCp₂)Dy(μ-Cl)]₂ (**3**) were carried out under strictly anaerobic and anhydrous conditions using an Ar filled glovebox (Vigor) and solvents dried and flushed with Ar using an SPS system (JC Meyer Solvent System). All glassware used in the glovebox was oven dried and cycled into the glovebox overnight. 2,6-bis(hydroxymethyl)pyridine and thionyl chloride were used to synthesize 2,6-bis(chloromethyl)pyridine and were purchased from Acros Organics and EMD Millipore, respectively. Anhydrous DyCl₃, NaCp (0.1 mol in THF), and anhydrous Dy(OTf)₃ were purchased from STREM. Elemental analyses were carried out by ALS Group USA. All syntheses were based on previously reported procedures.^{S1-S2} Samples used for magnetic characterization were either single crystalline material or microcrystalline powders prepared by dissolving materials in minimal amounts of DCM or THF followed by the addition of hexanes and placing in a freezer (-30 °C) overnight. Magnetic samples of **1**, **2**, and **3** were prepared with an eicosane matrix in a high purity NMR tube which was flame sealed under vacuum. The eicosane (Acros Organics) was melted in a hot water bath (45 °C) and was dispersed homogeneously throughout the sample. Magnetic characterization of **1**, **2**, and **3** as well as magnetically dilute analogues of **1** and **3** were obtained using a Quantum Design MPMS 3 SQUID magnetometer. DC measurements were acquired under an applied 1000 Oe field at a temperature range of 2-300 K. Variable temperature AC measurements for all compounds were taken under zero applied DC field at temperature ranges of 15-1.8 K with 2 Oe switching fields. ¹H NMR spectra were collected on Mercury 300 MHz spectrometer.

Crystallography

Data Collection. A Leica MZ 75 microscope was used to identify a suitable colorless crystal (for **1**: plate with dimensions (max, intermediate, and min) 0.185 x 0.14 x 0.138 mm³; for **2**: plate with dimensions 0.216 x 0.141 x 0.137 mm³; for **3**: needle with dimensions 0.142 x 0.023 x 0.022 mm³; for **3(thf)**: plate with dimensions 0.112 x 0.039 x 0.009 mm³) with very well defined faces from a representative sample of crystals of the same habit. The crystal mounted on a nylon loop was then placed in a cold nitrogen stream (Oxford) maintained at 110 K (100 K for **3(thf)**). A BRUKER APEX 2 Duo X-ray (three-circle) diffractometer was employed for crystal screening, unit cell determination, and data collection for **1**, **2**, and **3** (for **3(thf)** BRUKER Venture X-ray (kappa geometry) diffractometer). The goniometer was controlled using the APEX2 software suite, v2008-6.0.^{S3} The sample was optically centered with the aid of a video camera such that no translations were observed as the crystal was rotated through all positions. The detector was set at 6.0 cm from the crystal sample (APEX2, 512x512 pixel). The X-ray radiation employed was generated from a Mo sealed X-ray tube ($K_{\alpha} = 0.70173\text{\AA}$) for **1**, **2**, and **3** and a Cu-I μ s X-ray tube ($K_{\alpha} = 1.5418\text{\AA}$) with a potential of 50 kV and a current of 1.0mA for **3(thf)**.

45 data frames were taken at widths of 1.0°. For **1** and **2**, these reflections were used in the auto-indexing procedure to determine the unit cell. A suitable cell was found and refined by nonlinear least squares and Bravais lattice procedures. The unit cell was verified by examination of the h k l overlays on several frames of data. No super-cell or erroneous reflections were observed. For **3**, the unit cell was determined using Cell_Now,^{S4} which showed twinning. A suitable cell was found and refined by nonlinear least squares and Bravais lattice procedures.

After careful examination of the unit cell, an extended data collection procedure (21 sets for **1**; 23 sets for **2**; 25 sets for **3**; 15 sets for **3(thf)**) was initiated using omega and phi scans.

Data Reduction, Structure Solution, and Refinement. Integrated intensity information for each reflection was obtained by reduction of the data frames with the program APEX2^{S3,S5} (including both the twin domains for **3**). The integration method employed a three dimensional profiling algorithm and all data were corrected

for Lorentz and polarization factors, as well as for crystal decay effects. Finally the data was merged and scaled to produce a suitable data set. The absorption correction program SADABS^{S6} was employed to correct the data for 1 and 2 for absorption effects (for 3: TWINABS^{S7} was employed to correct the data for absorption effects as well as to generate TWIN4.hkl containing only the major component, and TWIN5.hkl with reflections from both the twin domains; while the former was used for structure solution the latter was used for the final least squares refinement).

Additional details for 1: Systematic reflection conditions and statistical tests of the data suggested the space group P-1. A solution was obtained readily using XT/XS in APEX2.^{S3, S5} Hydrogen atoms were placed in idealized positions and were set riding on the respective parent atoms. All non-hydrogen atoms were refined with anisotropic thermal parameters. Absence of additional symmetry and voids were confirmed using PLATON (ADDSYM).^{S8} CHECKCIF suggested pseudo-merohedral twinning and was included in the refinement. The structure was refined (weighted least squares refinement on F²) to convergence.^{S5, S9}

Olex2 was employed for the final data presentation and structure plots.^{S9}

Additional details for 2: Systematic reflection conditions and statistical tests of the data suggested the space group P-1. A solution was obtained readily using XT/XS in APEX2.^{S3, S5} Hydrogen atoms were placed in idealized positions and were set riding on the respective parent atoms. All non-hydrogen atoms were refined with anisotropic thermal parameters. Absence of additional symmetry and voids were confirmed using PLATON (ADDSYM).^{S8} The structure was refined (weighted least squares refinement on F²) to convergence.^{S5, S9} Olex2 was employed for the final data presentation and structure plots.^{S9}

Additional details for 3: Systematic reflection conditions and statistical tests of the data suggested the space group P2₁/n. A solution was obtained readily (Z=2; Z'=0.5) using XT/XS in APEX2.^{S3, S5} Dichloromethane was found partially solvated. Hydrogen atoms were placed in idealized positions and were set riding on the respective parent atoms. All non-hydrogen atoms were refined with anisotropic thermal parameters. Occupancy of the solvent dichloromethane were refined to 0.882. Absence of additional symmetry and voids were confirmed using PLATON (ADDSYM).^{S8} The structure was refined (weighted least squares refinement on F²) to convergence.^{S5, S9}

Additional details for 3(thf): Systematic reflection conditions and statistical tests of the data suggested the space group Pnnm. A solution was obtained readily (Z=2; Z'=0.25) using XT/XS in APEX2.^{S3, S5} A molecule of THF was found solvated and partially occupied. Hydrogen atoms were placed in idealized positions and were set riding on the respective parent atoms. All non-hydrogen atoms were refined with anisotropic thermal parameters. Elongated thermal ellipsoid on C2S suggested disorder and was successfully modeled between two positions. Considering symmetry and disorder, initial occupancy refinement suggested 1/4th occupancy for C2S and was fixed to that value for the final least squares refinement. Absence of additional symmetry or void were confirmed using PLATON (ADDSYM).^{S8} The structure was refined (weighted least squares refinement on F²) to convergence.^{S5, S9}

Synthesis of 2,6-bis(chloromethyl)pyridine: (similar to previous method^{S2}) 2,6-bis(hydroxymethyl)pyridine (10 g, 71.8 mmol) was weighed out in a 100 ml Schlenk flask and thionyl chloride (50 ml) was added dropwise while stirring at 0 °C. The solution was heated to 60 °C and stirred for 3 h. The reaction was cooled and added dropwise to 1 L of stirring ice water. The solution was neutralized with aqueous ammonia (25 %, EMD Milipore), and the white precipitate collected was washed extensively with water followed by vacuum drying. The solid was recrystallized from absolute ethanol/water (2:1 v:v) and the white needles were vacuum dried overnight prior to use for further reactions (11.9 g, 94%). ¹H NMR (300 MHz, CDCl₃) δ 7.77 ppm (1H, t, J = 6 Hz, py-H4), 7.45 ppm (2H, dd, J = 6 Hz, py-H3, H5), 4.66 ppm (4H, s, methylene).

Synthesis of 2,6-bis(methylenecyclopentadienyl)pyridine disodium salt ((PyCp₂)Na₂): (similar to previous method^{S2}) To a stirring solution of NaCp (0.1 mol) in 100 ml THF, a solution of 2,6-bis(chloromethyl)pyridine (4.4010 g, 0.025 mmol) in 150 ml THF was slowly added over time using an

addition funnel. This solution was stirred overnight and the reaction was filtered to remove the white precipitate and washed with THF (3 X 25 ml). The orange filtrate was evaporated down to approximately 80 ml and hexanes (150 ml) was slowly added to the solution and set aside overnight. The white crystals were collected by filtration, washed with hexanes (3 X 50 ml), and dried under vacuum to yield 3.1000 g (44 %). ¹H NMR (300 MHz, THF-d8) δ 7.42 ppm (1H, t, J = 6 Hz, py-H4), 6.92 ppm (2H, d, J = 9 Hz, py-H3,H5), 5.55 ppm (4 H, t, J = 3 Hz, Cp protons), 5.36 ppm (4 H, t, J = 3 Hz, Cp protons), 3.95 ppm (4 H, s, methylene).

Synthesis of [(PyCp₂)Dy(μ-OTf)]₂ (1): To a solution of Dy(OTf)₃ (1.2194 g, 2.00 mmol) in 30 ml of THF, a solution of (PyCp₂)Na₂ (0.5460 g, 2.00 mmol) in 60 ml of THF was added dropwise and kept in a cold well at -30 °C. The reaction was occasionally stirred manually for 2 h and warmed to room temperature. After 2 d of stirring, the THF was removed and replaced with DCM (30 ml) and left to stir overnight. The reaction was filtered and hexanes (50 ml) was slowly added to the filtrate and left overnight. Pale yellow crystals (0.125 g) were collected and the remaining mother liquor was collected and solvent removed. This was redissolved in DCM, layered with hexanes, and placed in a freezer (-30 °C) overnight to collect more crystals. The total yield was 0.3589 g (33 %). Anal. Calcd. for C₃₆H₃₀Dy₂F₆N₂O₆S₂ (**1**): C, 39.68; H, 2.77; N, 2.57. Found: C, 39.84; H, 2.73; N, 2.54.

Synthesis of [(PyCp₂)Dy(thf)(OTf)] (2): Approximately 50 mg of **3** was dissolved in 2 ml of THF and layered with 5 ml of hexanes and placed in a freezer (-30 °C) overnight. The resulting colorless plates were collected for further characterization. Anal. Calcd. for C₂₀H₁₉DyF₃NO_{3.5}S (**2**-(0.5 thf)): C, 41.35; H, 3.30; N, 2.41. Found: C, 40.91; H, 3.10; N, 2.46.

Synthesis of [(PyCp₂)Dy(μ-Cl)]₂ (3): The preparation followed the previously reported method for the isolation of **3**.³² To a suspension of DyCl₃ (0.5095 g, 1.895 mmol) in 50 ml of THF, a solution of (PyCp₂)Na₂ (0.5293 g, 1.895 mmol) in 60 ml of THF was added dropwise and kept in a cold well at -30 °C. The reaction was occasionally stirred manually for 2 h and warmed to room temperature. After 2 d of stirring, the reaction was filtered through Celite and the THF was removed and replaced with DCM (30 ml) and stirred overnight. The reaction was filtered through Celite and hexanes (50 ml) was slowly added to the filtrate and left overnight. The white microcrystalline material was collected and dried, 0.3334 g (40 %). Dissolving crystalline material of **3** in thf and crystallization via slow diffusion of hexanes into the solution resulted in the formation of plate crystals of **3**(thf).

Synthesis of magnetically dilute 1 [(PyCp₂)Ln(μ-OTf)]₂ (Dy : Y = 1 : 11.9). A magnetically dilute sample of **1** was prepared by dissolving 60.7 mg (63.3 μmol) of [(PyCp₂)Y(μ-OTf)] and 5.8 mg (5.3 μmol) of **1** in a minimal amount of CH₂Cl₂. The solution of **1** was added to the solution of [(PyCp₂)Y(μ-OTf)]₂, layered with hexanes, and left in a freezer at -30 °C overnight to form crystals suitable to conduct magnetic measurements. Unit cell parameters determined for single crystals of the dilute sample matched those of **1**.

Synthesis of magnetically dilute 3 [(PyCp₂)Ln(μ-Cl)]₂ (Dy : Y = 1 : 12). A magnetically dilute sample of **3** was prepared by dissolving 35.9 mg (49.1 μmol) of [(PyCp₂)Y(μ-Cl)]₂ and 3.6 mg (4.1 μmol) of **3** in a minimal amount of CH₂Cl₂. The solution of **3** was added to the solution of [(PyCp₂)Y(μ-Cl)]₂, layered with hexanes, and left in a freezer at -30 °C overnight to form crystals suitable to conduct magnetic measurements. Unit cell parameters determined for single crystals of the dilute sample matched those of **3**.

Computational Details.

Ab initio calculations were performed on compounds **1**, **2**, and **3** utilizing the MOLCAS 8.0 suite of computational chemistry programs.^{S10} All atom positions for each compound were provided to the GATEWAY module from solved and refined single crystal structures. Douglas–Kroll Hamiltonian^{S11} was considered to account for the relativistic effects. 1-electron velocity integrals and 1-electron atomic mean field integrals were computed with the SEWARD module, along with the 2-electron integrals which were Cholesky-decomposed. All the atomic basis sets used were of the ANO-RCC type^{S12} with the following contractions: hydrogen (2s), carbon, nitrogen, oxygen, and sulfur (3s2p1d), fluorine (3s2p), chlorine (5s4p2d1f), lutetium (7s6p4d2f) (used as a diamagnetic place-holder for one dysprosium atom in the dimers), and dysprosium (8s7p5d3f2g1h). The integrals computed were further used to develop starting orbitals for the compounds, by way of the GUESSORB module. A Complete Active Space Self-Consistent Field (CASSCF)^{S13} calculation was implemented with an active space of the seven f-orbitals of dysprosium Dy(III) containing nine electrons, using the RASSCF module. The twenty-one sextet roots of dysprosium Dy(III) were found through the configuration interaction procedure enacted by this module and then the resulting twenty-one states were mixed by the RASSI module. The RASSI module was then used to determine the interactions between the twenty-one roots, while taking into account spin-orbit coupling.^{S14} The output from RASSI was subsequently used by the SINGLE_ANISO module^{S15} to compute the magnetic properties (g-tensors and single-ion energy barrier) based on the eight low-lying Kramers doublet (KDs). for the compounds featured in this paper.

To model the exchange and dipolar coupling present in the chloride (**1**) and triflate (**3**) dimer compounds, the POLY_ANISO program^{S16-S18} was utilized by producing fits to the DC magnetic susceptibility data for the two compounds ($zJ = -0.01 \text{ cm}^{-1}$ for **1** and **3**).

The magnetic couplings of compounds **1** and **3** are extracted using the following Hamiltonian.

$$\hat{H}_{coupling} = -(J_i S_i S_{i+1}) \quad \dots\dots\dots \text{Eq.1}$$

(here $J_i = J_i^{dipolar} + J_i^{exch}$; i.e. J_i are the total magnetic interaction in combination of calculated $J_i^{dipolar}$ and fitted J_i^{exch} parameters; this describes the interaction between the intramolecular metal centres.)

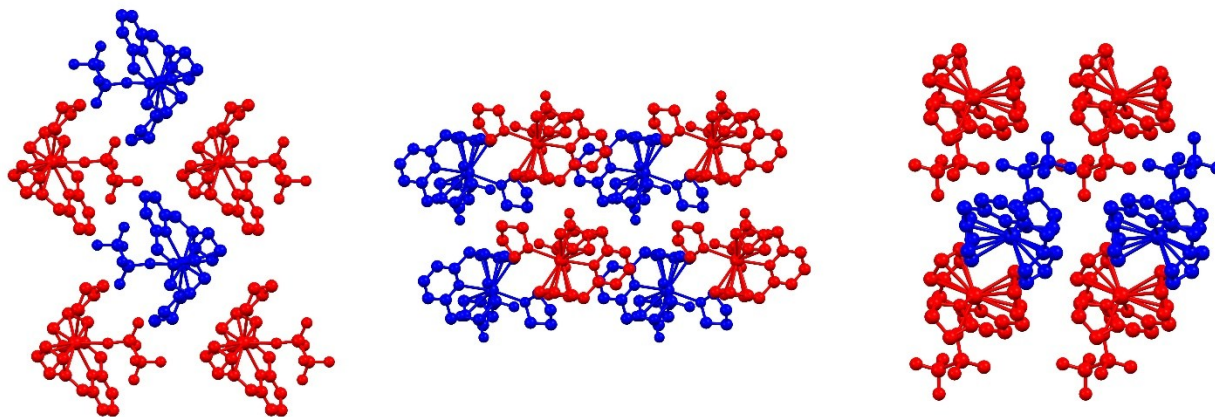


Fig. S1 Packing diagram for **2** viewing along a-(left), b-(center), and c-axis (right).

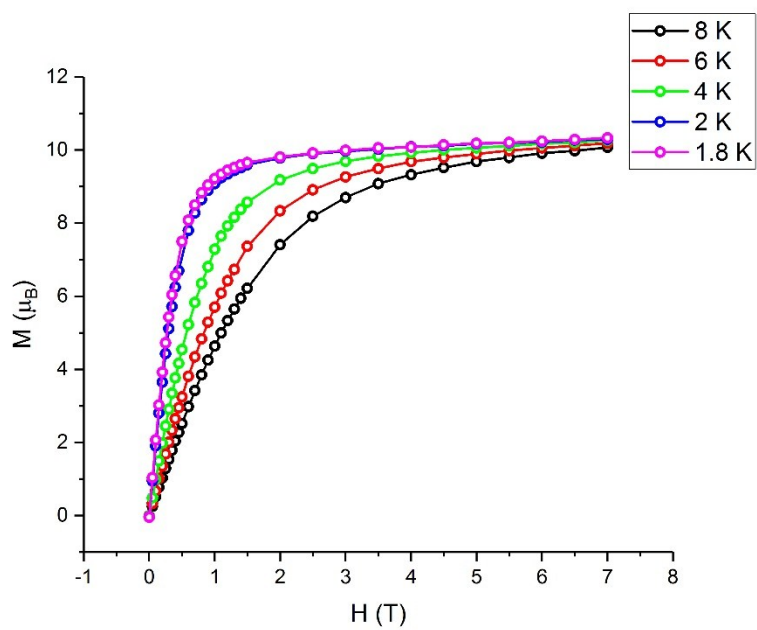


Fig. S2 Plot of Magnetization vs. Field at 8-1.8 K for **1**.

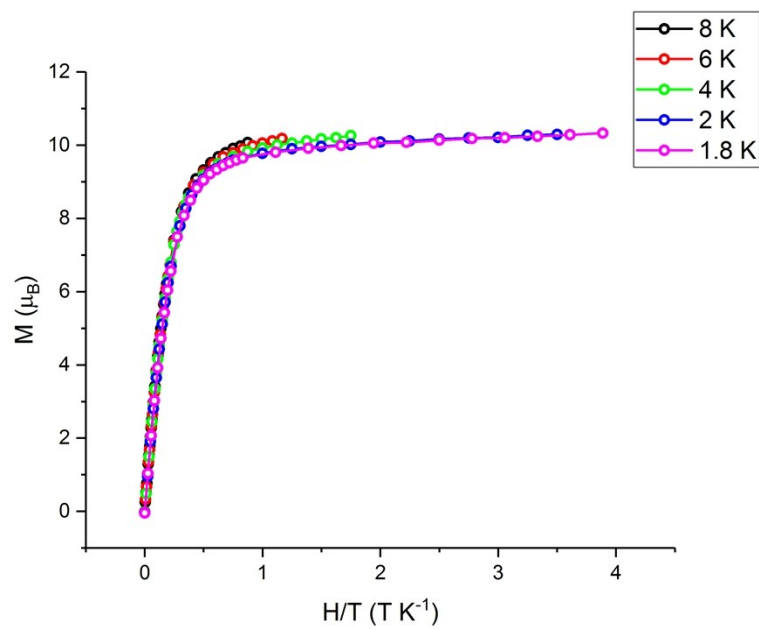


Fig. S3 Plot of Magnetization vs. H/T at 8-1.8 K for **1**.

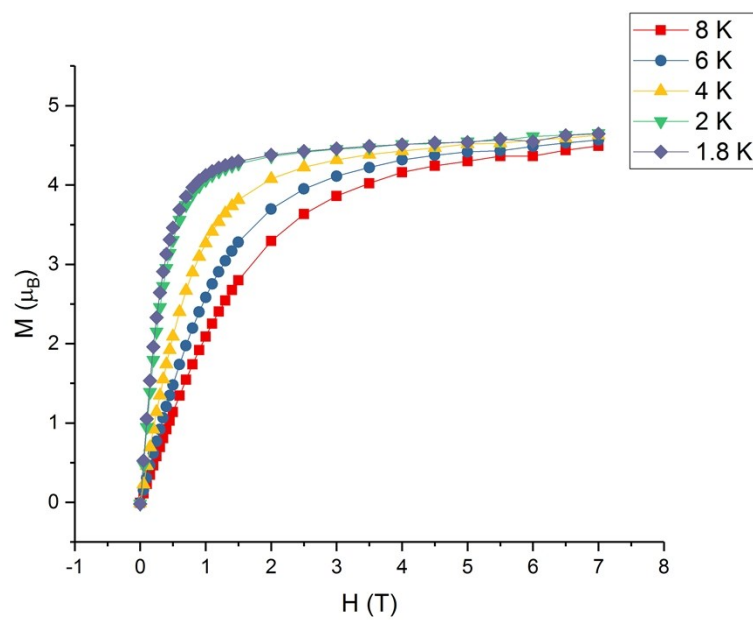


Fig. S4 Plot of Magnetization vs. Field at 8-1.8 K for **2**.

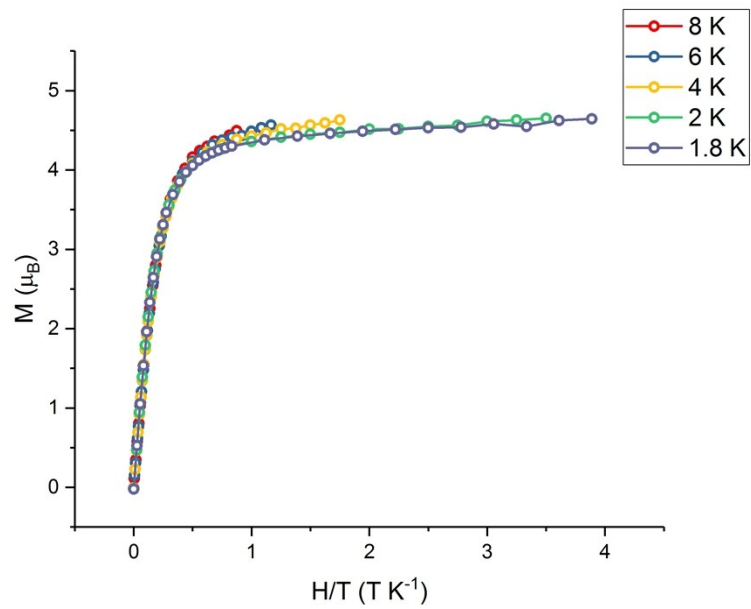


Fig. S5 Plot of Magnetization vs. H/T at 8-1.8 K for **2**.

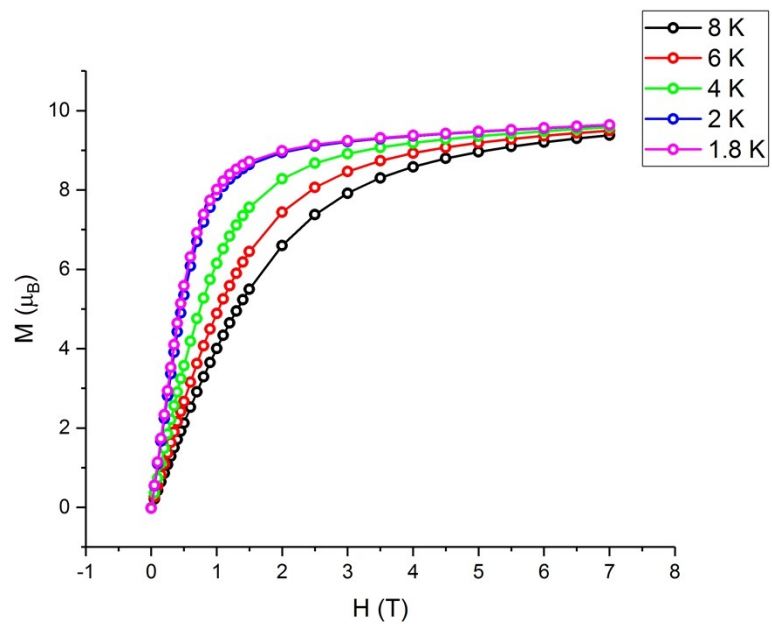


Fig. S6 Plot of Magnetization vs. Field at 8-1.8 K for **3**.

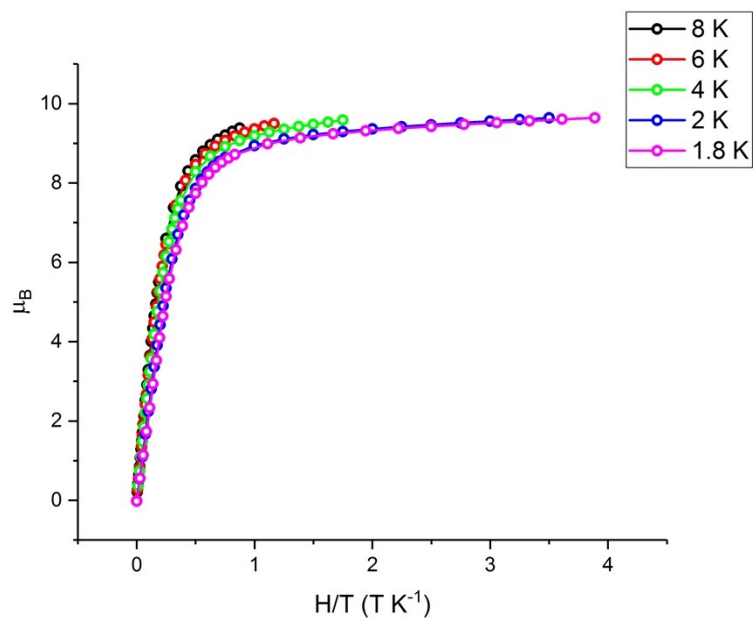


Fig. S7 Plot of Magnetization vs. H/T at 8-1.8 K for **3**.

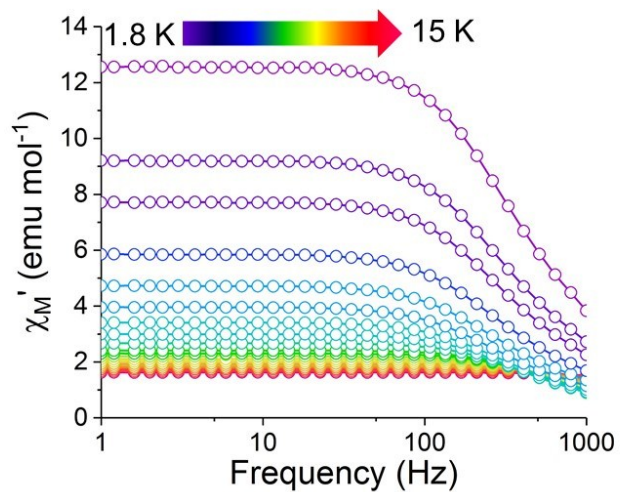


Fig. S8 Frequency dependence of the in-phase component (χ_M') of the ac susceptibility of **1** under 0 Oe applied dc field in the temperature range 1.8 – 15 K.

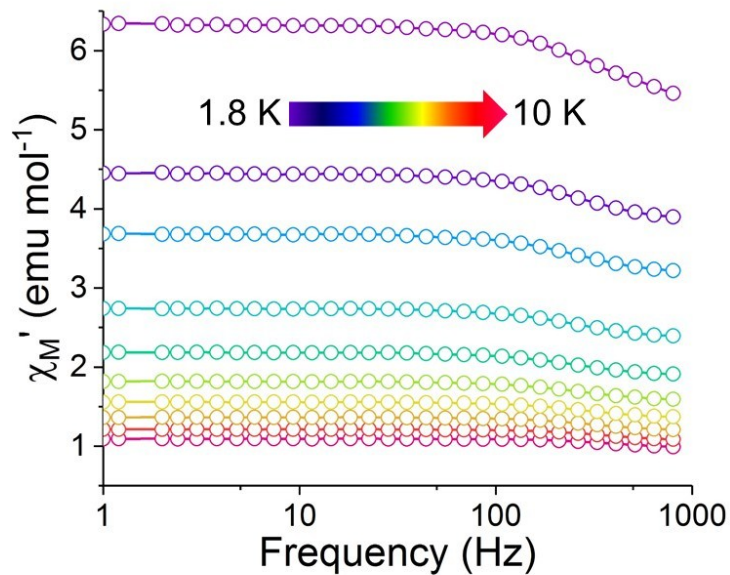


Fig. S9 Frequency dependence of the in-phase component (χ_M') of the ac susceptibility of **2** under 0 Oe applied dc field in the temperature range 1.8 – 10 K

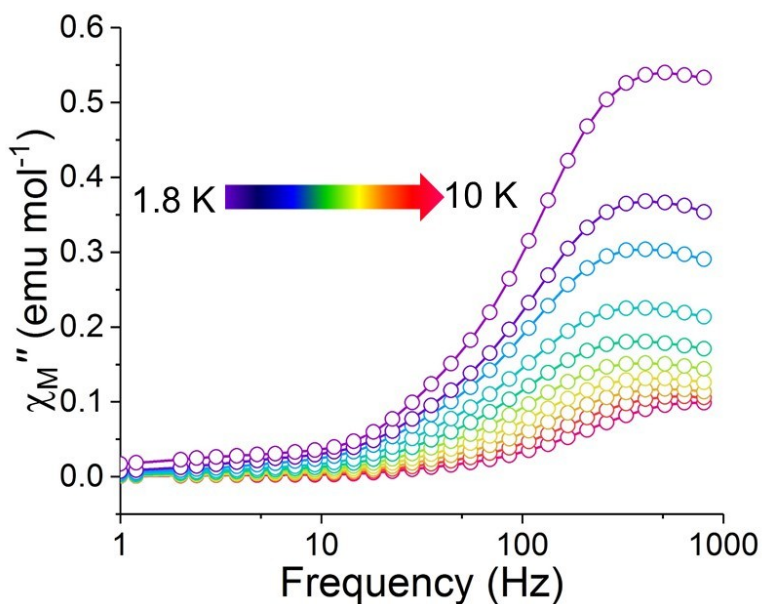


Fig. S10 Frequency dependence of the out-of-phase component (χ_M'') of the ac susceptibility of **2** under 0 Oe applied dc field in the temperature range 1.8 – 10 K.

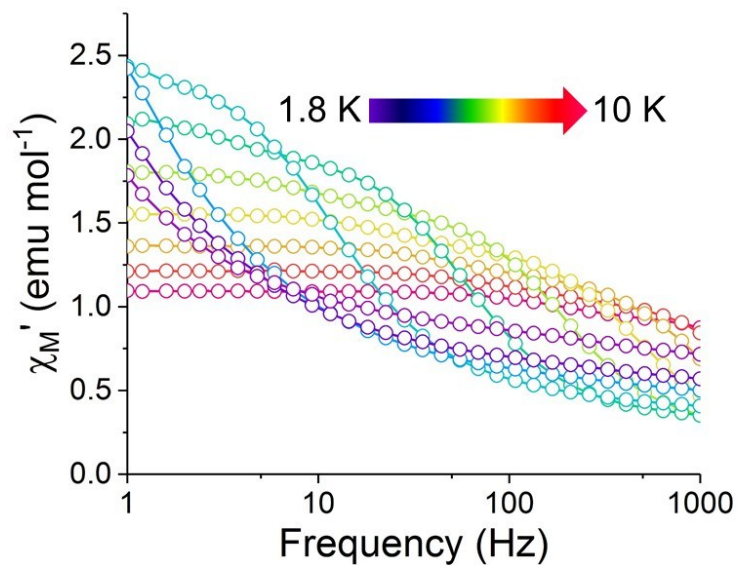


Fig. S11 Frequency dependence of the in-phase component (χ_M') of the ac susceptibility of **2** under 1000 Oe applied dc field in the temperature range 1.8 – 15 K

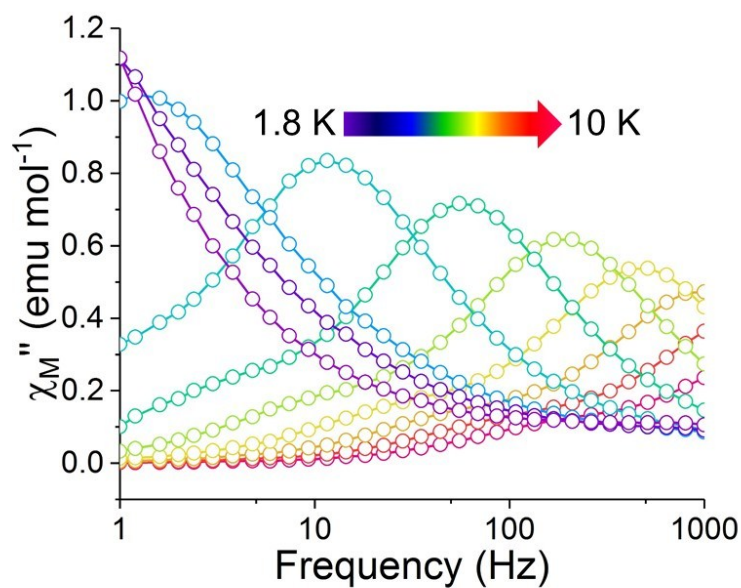


Fig. S12 Frequency dependence of the out-of-phase component (χ_M'') of the ac susceptibility of **2** under 1000 Oe applied dc field in the temperature range 1.8 – 15 K

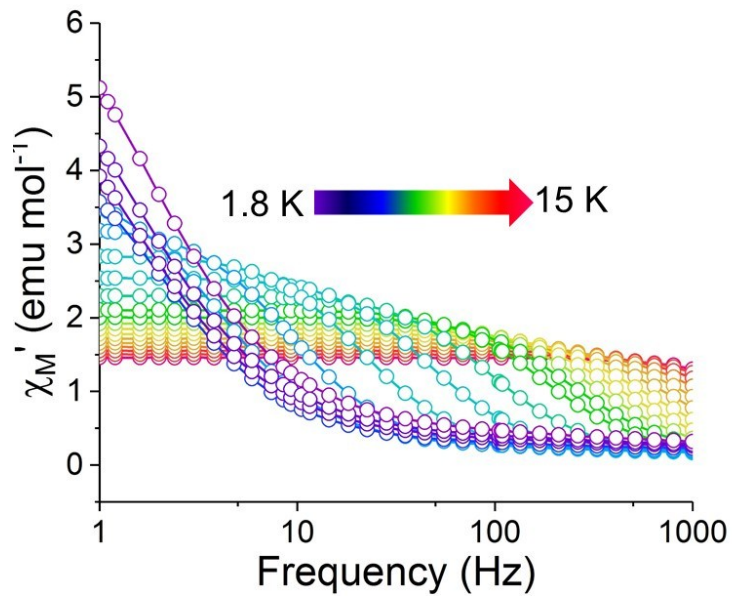


Fig. S13 Frequency dependence of the in-phase component (χ_M') of the ac susceptibility of **3** under 0 Oe applied dc field in the temperature range 1.8 – 15 K.

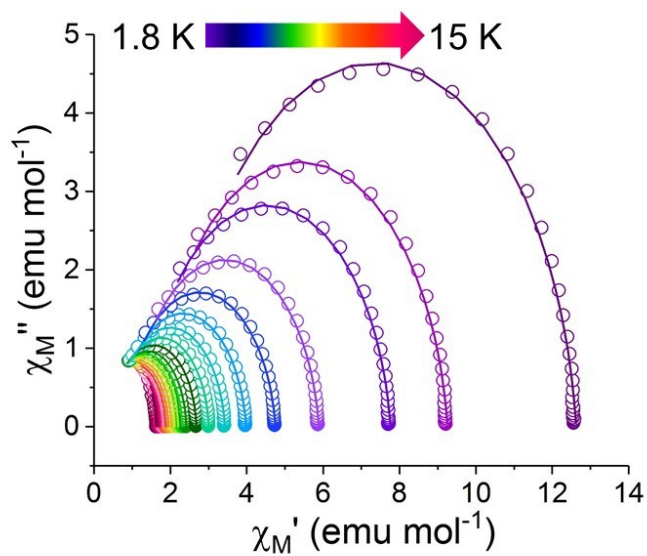


Fig. S14 Cole-Cole plots under zero dc field for **1**. Solid lines are the best fits to the experimental data, obtained with the generalized Debye model.

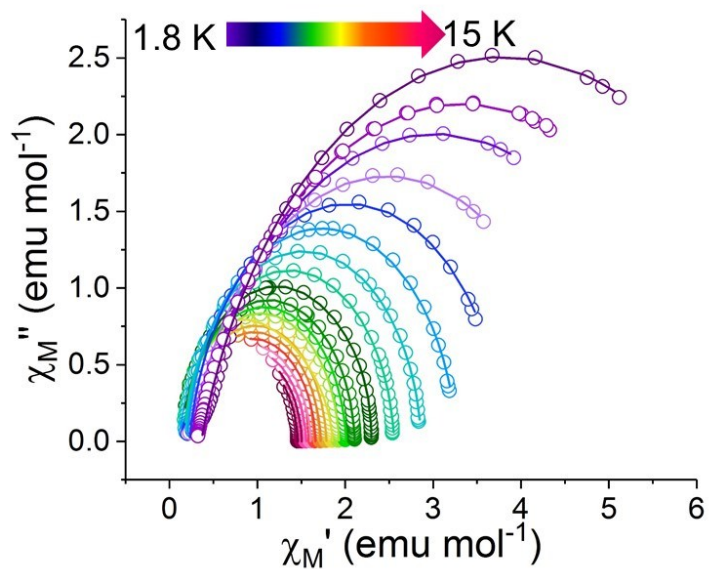


Fig. S15 Cole-Cole plots under zero dc field for **3**. Solid lines are the best fits to the experimental data, obtained with the generalized Debye model.

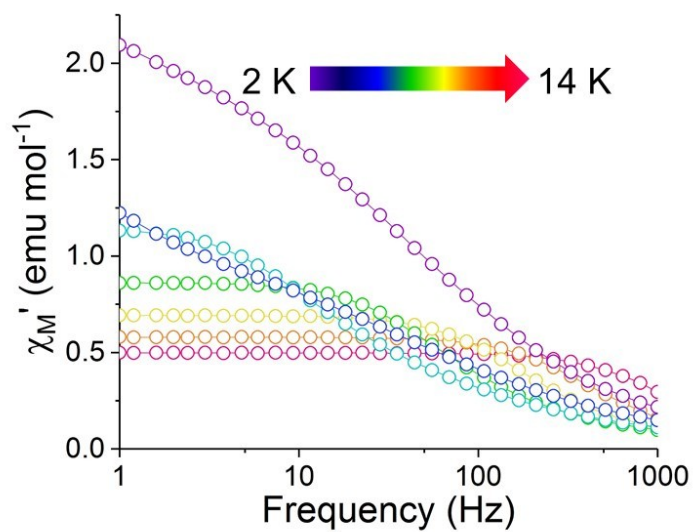


Fig. S16 Frequency dependence of the in-phase component (χ_M') of the ac susceptibility of **magnetically dilute 1** under 0 Oe applied dc field in the temperature range 2 – 14 K.

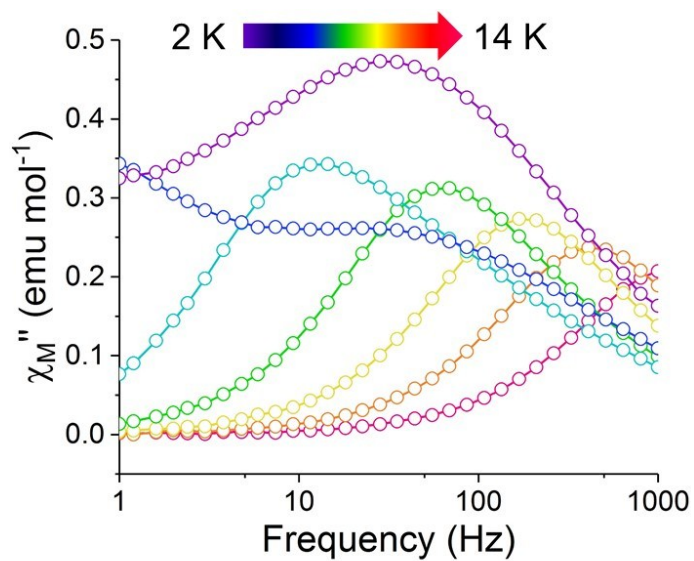


Fig. S17 Frequency dependence of the out-of-phase component (χ_M'') of the ac susceptibility of **magnetically dilute 1** under 0 Oe applied dc field in the temperature range 2 – 14 K.

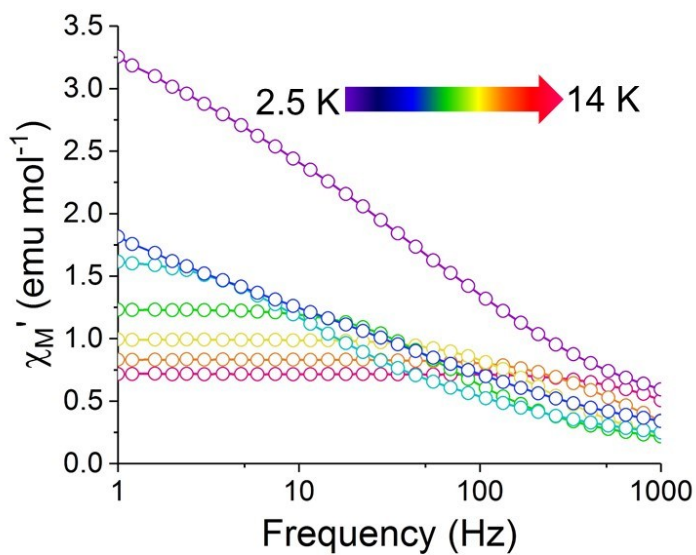


Fig. S18 Frequency dependence of the in-phase component (χ_M') of the ac susceptibility of **magnetically dilute 3** under 0 Oe applied dc field in the temperature range 2.5 – 14 K.

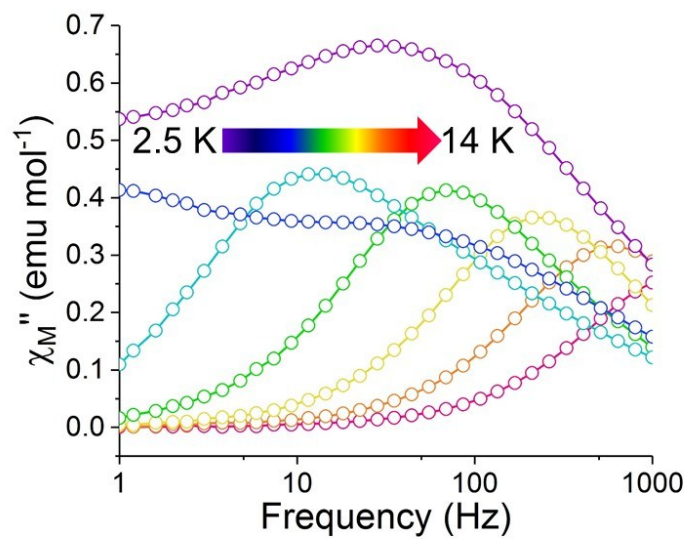


Fig. S19 Frequency dependence of the out-of-phase component (χ_M'') of the ac susceptibility of magnetically dilute 3 under 0 Oe applied dc field in the temperature range 2.5 – 14 K.

Table S1. Crystallographic Data for **1**, **2**, **3**, and **3(thf)**.

Compound	1·2CH₂Cl₂	2	3·0.88CH₂Cl₂	3(thf)
Formula	C ₃₈ H ₃₄ Cl ₄ Dy ₂ F ₆ N ₂ O ₆ S ₂	C ₂₂ H ₂₃ DyF ₃ NO ₄ S	C _{35.76} H _{33.53} Cl _{5.53} Dy ₂ N ₂	C ₃₈ H ₃₈ Cl ₂ Dy ₂ N ₂ O
Crystal system	triclinic	triclinic	monoclinic	orthorhombic
Space group	P-1	P-1	P2 ₁ /n	Pnmm
a, Å	12.259(1)	8.2141(3)	14.876(1)	18.8766(7)
b, Å	13.208(1)	11.0008(4)	7.1590(7)	7.3260(3)
c, Å	13.751(1)	12.1504(5)	16.663(2)	13.6863(5)
α, °	92.254(4)	82.426(2)	90	90
β, °	90.145(4)	78.374(2)	92.235(4)	90
γ, °	107.140(4)	88.147(2)	90	90
Volume, Å ³	2096.9(3)	9937.9(14)	1773.3(3)	1892.7(1)
Z	2	2	2	2
T, K	110	110	110	100
ρ _{calcd} (mg/m ³)	1.995	1.922	1.896	1.640
F(000)	1220	606	976	908
Θ _{min} , Θ _{max} , °	1.482, 25	1.725, 27.644	3.908, 62.443	3.989, 61.498
R ₁ ^a , wR ₂ ^b (I > 2σ(I))	0.0617, 0.1560	0.0149, 0.0361	0.0678, 0.1748	0.0687, 0.1460
R ₁ ^a , wR ₂ ^b (all data)	0.0773, 0.1690	0.0169, 0.0373	0.0831, 0.1845	0.0820, 0.1553

^aR₁ = 3||F_o|-|F_c||/3|F_o|. ^bwR₂ = [3[w(F_o² - F_c²)²]/3[w(F_o²)²]]^{1/2}, w = 1/σ²(F_o²) + (aP)² + bP, where P = [max(0 or F_o²) + 2(F_c²)]/3.

Table SX. Selected bond lengths and angles in molecular **structures of 1, 2, and 3.**

	1	2	3
Dy-C, A (range)	2.591(11) - 2.657(13) 2.603(12) - 2.670(13)	2.587(2) - 2.669(2)	2.61(1) - 2.68(1)
Dy-N, A	2.562(9) 2.546(9)	2.5375(16)	2.581(9)
Dy-O, A (triflate)	2.322(9), 2.354(8) 2.315(8), 2.376(8)	2.3352(14)	-
Dy-O, A (thf)	-	2.4560(13)	-
O-Dy-O,	75.4(3) 75.6(3)	72.99(5)	-
Dy-Cl, A	-	-	2.683(3), 2.785(3)
Cl-Dy-Cl,	-	-	77.94(9)

Table S3. Calculated g-tensor for Kramer's doublets of individual Dy sites in **1**, **2**, and **3**.

Kramers doublet	g-tensor components	1		2	3	
		Dy 1	Dy 2	Dy	Dy 1	Dy 2
1	g_x	0.0083	0.0083	0.0995	0.0081	0.0082
	g_y	0.0250	0.0249	0.2004	0.0226	0.0227
	g_z	19.3038	19.2283	18.7695	19.0501	19.1629
2	g_x	1.2368	1.2365	0.2639	0.2529	0.2543
	g_y	6.7989	6.7729	0.9190	0.9696	0.9741
	g_z	12.5748	12.5515	17.9002	15.9790	16.0269
3	g_x	0.6673	0.6575	7.5583	2.8529	2.8664
	g_y	3.8125	3.8120	7.1917	3.3862	3.4131
	g_z	7.3693	7.3392	4.0711	14.1677	14.2213
4	g_x	2.8646	2.8650	3.8984	2.1680	2.1828
	g_y	4.4304	4.4306	4.9813	3.8553	3.8731
	g_z	10.8902	10.8632	8.5726	12.2455	12.2824
5	g_x	1.5013	1.4897	0.8492	0.6206	0.6193
	g_y	1.6700	1.6659	4.0447	1.0619	1.0724
	g_z	15.0689	15.0696	9.5789	15.5567	15.5648
6	g_x	8.6380	8.6308	4.8145	8.2151	8.2826
	g_y	6.9324	6.9118	5.9396	7.9019	7.9017
	g_z	3.3646	3.3529	7.8326	3.6546	3.6824
7	g_x	0.2139	0.2097	1.0721	0.1068	0.1122
	g_y	0.9202	0.9192	1.8331	2.1232	2.1333
	g_z	15.7195	15.6790	13.7933	13.1789	13.2285
8	g_x	0.4479	0.4472	0.0298	1.0347	1.0348
	g_y	1.3712	1.3659	1.1715	2.9454	2.9674
	g_z	17.4861	17.4602	16.8567	16.3088	16.4083

Table S4. Lowest exchange doublets arising from magnetic coupling and the corresponding tunnel splitting and g_z value of each doublet (g_x and $g_y = 0$) for complex **1**. Bold indicates doublet through which magnetic relaxation is expected to occur.

#	Energy (cm ⁻¹)	Tunneling splitting (cm ⁻¹)	g_z
1	0.000000000000 0.000001275082	1.28×10^{-6}	38.532
2	0.239069593853 0.239071092639	1.50×10^{-6}	0.081
3	138.005807071743 138.006292097241	4.85×10^{-4}	31.648
4	138.127649799422 138.133378788417	5.73×10^{-3}	28.514
5	138.154082220392 138.159893316113	5.81×10^{-3}	0.368
6	138.274405289145 138.275070635627	6.65×10^{-4}	0.232

Table S5. Lowest exchange doublets arising from magnetic coupling and the corresponding tunnel splitting and g_z value of each doublet (g_x and $g_y = 0$) for complex **3**. Bold indicates doublet through which magnetic relaxation is expected to occur.

#	Energy (cm ⁻¹)	Tunneling splitting (cm ⁻¹)	g_z
1	0.000000000000 0.000001593754	1.59×10^{-6}	0.130
2	1.582867138374 1.582869352357	2.21×10^{-6}	38.211
3	133.742118771048 133.742136639318	1.79×10^{-5}	0.102
4	133.953725623240 133.953815131459	8.95×10^{-5}	0.082
5	135.098096546347 135.098169984440	7.34×10^{-5}	35.068
6	135.247962328973 135.248102733045	1.40×10^{-4}	35.070

References

- S1 G. Paolucci, J. Zanon, V. Lucchini, W. E. Damrau, E. Siebel and D. R. Fischer, *Organometallics*, 2002, **21**, 1088-1094.
- S2 G. Paolucci., R. D'Ippolito, C. Ye, C. Qian, J. Gräper and D. R. Fischer, *Journal of Organometallic Chemistry*, 1994, **471**, 97-104.
- S3 APEX2 "Program for Data Collection on Area Detectors" BRUKER AXS Inc., 5465 East Cheryl Parkway, Madison, WI 53711-5373 USA
- S4 Sheldrick, G. M. "Cell_Now (version 2008/1): Program for Obtaining Unit Cell Constants from Single Crystal Data": University of Göttingen, Germany
- S5 Sheldrick, G.M. (2008). *Acta Cryst. A*64, 112-122. Sheldrick, G. M. (2015), *Acta Cryst. A*71, 3-8. Sheldrick, G. M. (2015). *Acta Cryst. C*71, 3-8. XT, XS, BRUKER AXS Inc., 5465 East Cheryl Parkway, Madison, WI 53711-5373 USA.
- S6 SADABS, Sheldrick, G.M. "Program for Absorption Correction of Area Detector Frames", BRUKER AXS Inc., 5465 East Cheryl Parkway, Madison, WI 53711-5373 USA
- S7 TWINABS, Sheldrick, G.M. "Program for Absorption Correction of Area Detector Frames", BRUKER AXS Inc., 5465 East Cheryl Parkway, Madison, WI 53711-5373 USA.
- S8 Spek, A. L., "PLATON - A Multipurpose Crystallographic Tool" *J. Appl. Cryst.* 2003, 36, 7-13.; Spek, A. L., Utrecht University, Utrecht, The Netherlands 2008.
- S9 O. V. Dolomanov, L. J. Bourhis, R. J. Gildea, J. A. K. Howard, and H. Puschmann, *J. Appl. Cryst.*, 2009, **42**, 339-341.
- S10 F. Aquilante, J. Autschbach, R. K. Carlson, L. F. Chibotaru, M. G. Delcey, L. De Vico, I. Fdez. Galván, N. Ferré, L. M. Frutos, L. Gagliardi, M. Garavelli, A. Giussani, C. E. Hoyer, G. Li Manni, H. Lischka, D. Ma, P. Å. Malmqvist, T. Müller, A. Nenov, M. Olivucci, T. B. Pedersen, D. Peng, F. Plasser, B. Pritchard, M. Reiher, I. Rivalta, I. Schapiro, J. Segarra-Martí, M. Stenrup, D. G. Truhlar, L. Ungur, A. Valentini, S. Vancoillie, V. Veryazov, V. P. Vysotskiy, O. Weingart, F. Zapata and R. Lindh, *J. Comp. Chem.* **2016**, *37*, 506-541.
- S11 Hess, B. A.; Marian, C. M.; Wahlgren, U.; Gropen, O. *Chem. Phys. Lett.* **1996**, *251*, 365-371.
- S12 B. O. Roos, R. Lindh, P.-Å. Malmqvist, V. Veryazov, P.-O. Widmark and A. C. Borin, *J. Phys. Chem. A*, 2008, **112**, 11431-11435.
- S13 B. O. Roos and P.-Å. Malmqvist, *Phys. Chem. Chem. Phys.*, 2004, **6**, 2919-2927.
- S14 P. Å. Malmqvist, B. O. Roos and B. Schimmelpfennig, *Chem. Phys. Lett.*, 2002, **357**, 230-240.
- S15 L. F. Chibotaru and L. Ungur, *J. Chem. Phys.* 2012, **137**, 064112-22.
- S16 L. F. Chibotaru, L. Ungur and A. Soncini, *Angew. Chem. Int. Ed.*, 2008, **47**, 4126-4129.
- S17 L. Ungur, W. Van den Heuvel and L. F. Chibotaru, *New J. Chem.*, 2009, **33**, 1224-1230.
- S18 L. F. Chibotaru, L. Ungur, C. Aronica, H. Elmoll, G. Pilet and D. Luneau *J. Am. Chem. Soc.*, 2008, **130**, 12445-12455.